Electronic Supplementary Material (ESI) for Chemical Communications.

Electronic Supplementary Information (ESI) for

Oxygen vacancy induced Bi_2WO_6 for the realization of photocatalytic CO_2 reduction over the full solar spectrum: from the UV to the NIR region

by

Xin Ying Kong, [a] Yen Yee Choo, [a] Siang-Piao Chai, *[a] Ai Kah Soh [b] and Abdul Rahman Mohamed [c]

[a] Multidisciplinary Platform of Advanced Engineering, Chemical Engineering Discipline, School of Engineering, Monash University, Jalan Lagoon Selatan, 47500 Bandar Sunway, Selangor, Malaysia.

[b] Multidisciplinary Platform of Advanced Engineering, Mechanical Engineering Discipline, School of Engineering, Monash University, Jalan Lagoon Selatan, 47500 Bandar Sunway, Selangor, Malaysia.

[c] Low Carbon Economy (LCE) Group, School of Chemical Engineering, Universiti Sains Malaysia, Engineering Campus, Seri Ampangan, 14300 Nibong Tebal, Penang, Malaysia.

* Corresponding author:

Tel: +603-5514 6234; Fax: +603-5514 6207

E-mail address: chai.siang.piao@monash.edu

(1) Detailed Experimental Procedures

Chemical reagents

All chemicals reagents were of analytical grade and were used as received without any further purification. Bismuth (III) nitrate pentahydrate, $Bi(NO_3)_3{\cdot}5H_2O$ (≥ 98.0%) and ethylene glycol, EG (≥ 99.0%) were purchased from Sigma Aldrich; sodium tungstate dihydrate, $Na_2WO_4{\cdot}2H_2O$ (≥ 99.0%) was supplied by Merck and ethanol, C_2H_5OH (Grade AR 96.0%) was procured from Friendemann Schmidt Chemical. Deionized (DI) water with resistivity ≥ 18 MΩ cm was utilized throughout the experiment.

Synthesis of photocatalysts

Bi_2WO_6 with oxygen vacancies was prepared *via* a highly facile one-step ethylene glycol-assisted solvothermal process. In brief, 2 mmol of $Na_2WO_4{\cdot}2H_2O$ was dissolved in 30 mL of EG and the homogenous solution was added dropwise into 70 mL of EG solution containing 4 mmol of $Bi(NO_3)_3{\cdot}5H_2O$. The colourless solution was vigorously stirred for 1 h at room temperature, and then transferred to a 125mL Teflon-lined stainless steel autoclave, which was maintained at 180^oC for 20 h under autogenous pressure. After completion of the reaction, the autoclave was air-cooled to room temperature and the resulting precipitate was collected and washed with ethanol and DI water for several times to remove residual ions. The final product was dried at 60^oC for overnight and was designated as Bi_2WO_6-OV. On another note, pristine Bi_2WO_6 without oxygen vacancy defects was obtained by annealing Bi_2WO_6-OV at 400^oC in air-rich atmosphere for 4 h to reoxidize the surface. The sample collected was denoted as Bi_2WO_6-P.

Material characterization

The surface morphology of the as-synthesized samples was investigated using a Hitachi SU8010 field emission scanning electron microscopy (FESEM). High resolution transmission electron microscopy (HRTEM) images were acquired by TECNAI G2 F20 transmission electron microscope at an accelerating voltage of 200 kV. The sample for TEM analysis was prepared by depositing the sample suspension in ethanol onto carbon-coated copper grid. The electron spin resonance (ESR) spectra of the samples were obtained by a JEOL JES-FA200 ESR spectrometer. Powder X-ray diffraction (XRD) patterns were recorded using a Bruker D8 Discover X-Ray diffractometer with Cu K_α radiation (λ = 0.15406 nm) at a scan rate of 0.02 s^{-1} with applied current and accelerating voltage of 40 mA and 40 kV, respectively. The Raman Spectra were obtained using a micro Raman spectrometer (Horiba LabRAM HR Evolution) at room temperature with 514 nm laser excitation. The high resolution X-ray photoelectron spectroscopy

(XPS) spectra were attained on a scanning X-ray microprobe PHI Quantera II (Ulvac-PHI, INC.) equipped with an monochromatic Al-K_α ($h\nu$ = 1486.6 eV) X-ray source and analysed under ultra-vacuum (2.4 x 10^{-6}) environment. All binding energies were charged corrected by adventitious carbon signal (C 1s peak) at 284.6 eV. The absorbance spectra of the photocatalysts were measured using Agilent Cary 100 ultraviolet-visible (UV-vis) spectrophotometer within the range of 200–800 nm and the bandgap energies were determined from Kubelka-Munk (KM) function, $F(R)$ and extrapolation of Tauc plots, $[F(R)\cdot h\nu]^{1/2}$ vs. $h\nu$.

Evaluation of photocatalytic CO_2 reduction

The photocatalytic activity of the as-prepared samples was evaluated by photoreduction of CO_2 into CH_4. The experiment was conducted at ambient temperature and atmospheric pressure in a custom-made, continuous gas flow reactor, as reported in our previous works.[1-6] A 500 W Xenon arc lamp (CHF-XM-500W) equipped with different cut-off filters was employed to provide multiple light source, including UV ($\lambda < 400$ nm), Vis ($\lambda > 400$ nm), NIR ($\lambda > 700$ nm) and simulated solar light (AM 1.5 filter). In a typical CO_2 photoreduction experiment, the photocatalysts were uniformly coated on glass rods and were placed into quartz columns. The CO_2 source of high purity (99.999%) was bubbled through H_2O to provide a gas mixture of CO_2 and water vapour (reactant gas), which was directed to the quartz columns to allow intimate contact between the reactant gas and photocatalysts. Prior to photoreaction, the reactant gas was purged through the reactor at a flowrate of 50 mL/min for 30 min to remove any excess air from the system and also to ensure reactant gas molecules were completely adsorbed on the surface of photocatalysts. Henceforth, the reactant gas flow rate was reduced to 5 mL/min and it was maintained for 8 h under different light irradiation to evaluate the photocatalytic activity of the as-prepared samples. The product gas was collected at every 1 h interval and analyzed by using a gas chromatography (Agilent 7820A GC), equipped with flame ionized detector (FID) and thermal conductivity detector (TCD). The experiment set-up is illustrated in Fig. S1 and this set-up was enclosed in a black box to avoid any light interference from the surroundings to the reaction environment. The CH_4 yield was quantified using Eq. S1.

$$\text{Yield}\ (\mu\text{mol g}^{-1}\text{h}^{-1}) = \frac{(C_{\text{final},CH_4} - C_{\text{initial},CH_4}) \times \text{volumetric flowrate of product gas}}{\text{Amount of photocatalyst used}} \qquad \text{(S1)}$$

Experimental set-up for photocatalytic CO_2 reduction

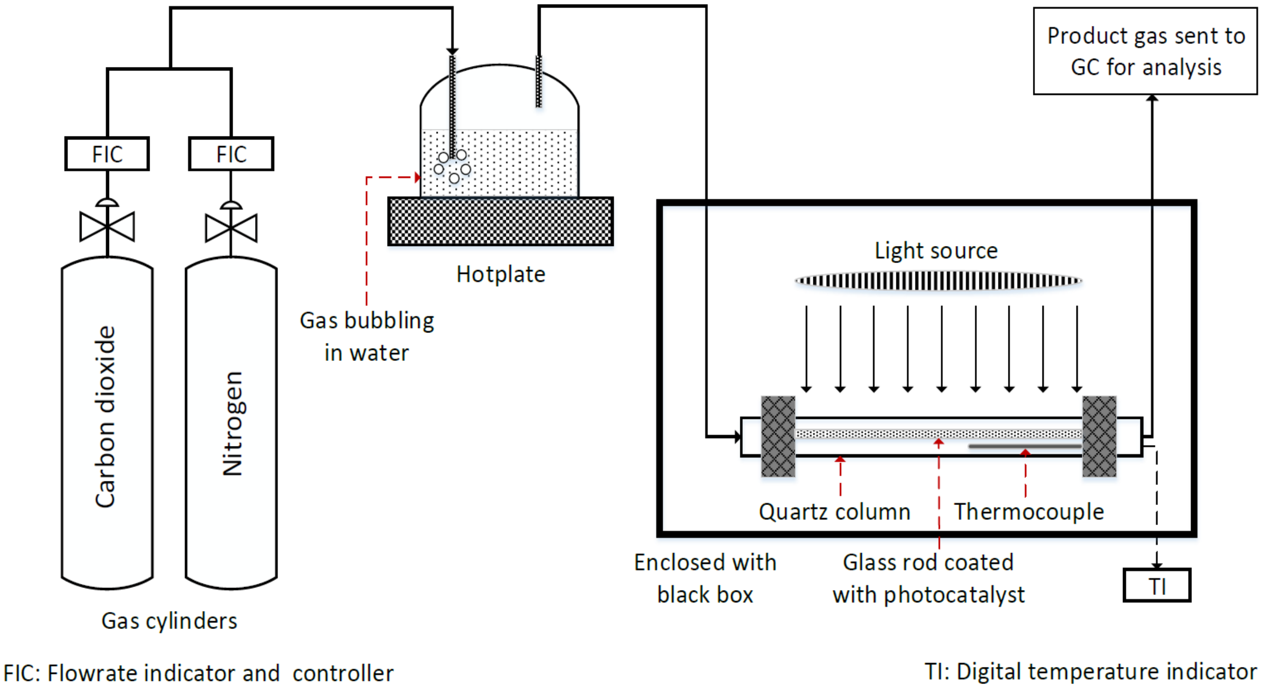

Figure S1 Schematic diagram of the set-up of photocatalytic CO_2 reduction experiment.

Control measurements of photocatalytic CO_2 reduction

To validate the indispensable role of Bi_2WO_6-OV and Bi_2WO_6-P as photocatalysts to drive the reduction of CO_2 to CH_4, a number of control experiments were performed, including: (1) under CO_2/H_2O vapour flow and light irradiation but without photocatalyst; (2) under CO_2/H_2O vapour flow with photocatalyst but without light irradiation; (3) under light irradiation with photocatalyst but without CO_2 (under N_2/H_2O vapour flow) and (4) under light irradiation with photocatalyst but without H_2O (under CO_2 flow only). In all these cases, negligible-to-none of CH_4 products was generated. Therefore, the product yields detected in the reactions could be confidently assigned to stem from photocatalytic CO_2 reduction and the possibility of the source of carbon residuals and photolysis could be ruled out. In addition, it was proven that photocatalyst, light source and CO_2/H_2O vapour flow are the several prerequisites for CO_2 photoreduction to take place.

(2) Structural Features of Bi_2WO_6-P

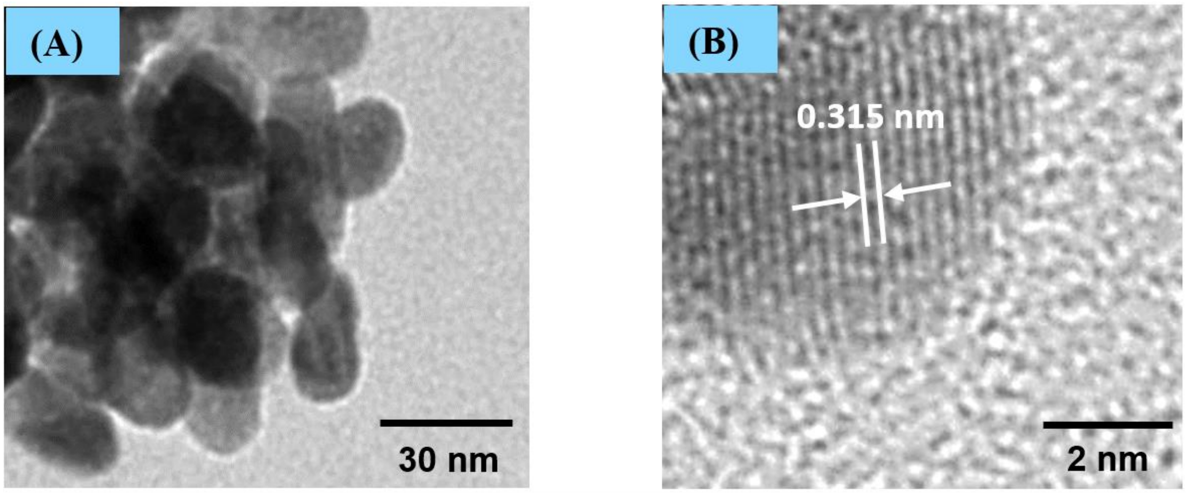

Figure S2 (A) TEM image and (B) HRTEM image of the as-developed Bi_2WO_6-P.

(3) High Resolution W 4f and O 1s XPS spectra

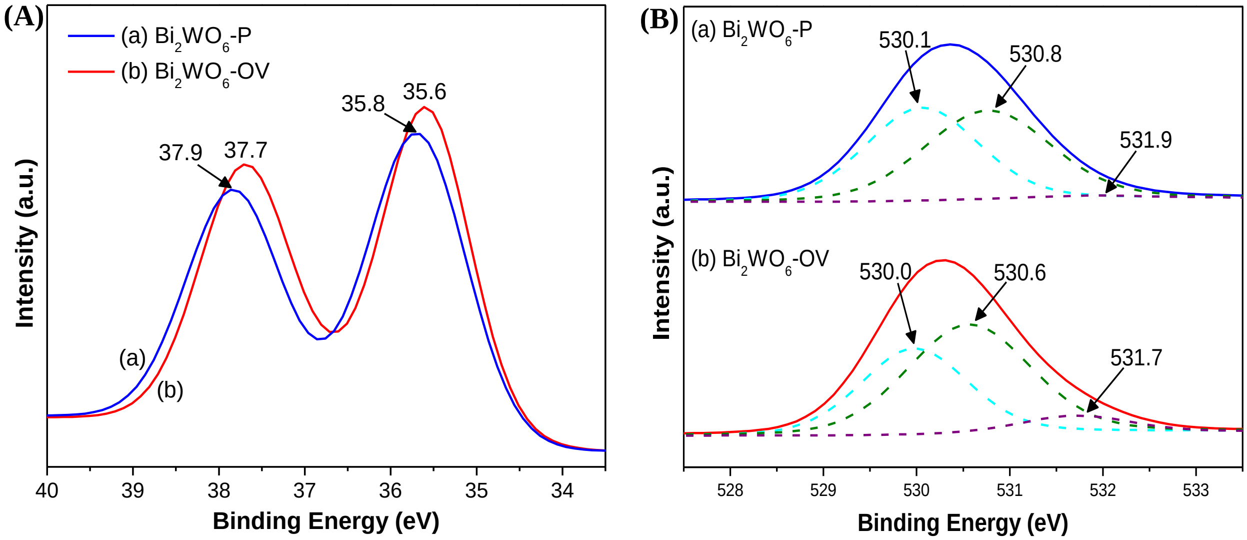

Figure S3 (A) High resolution W 4f and O 1s XPS spectra of Bi_2WO_6-P and Bi_2WO_6-OV.

(4) Stability Test of Bi_2WO_6-OV

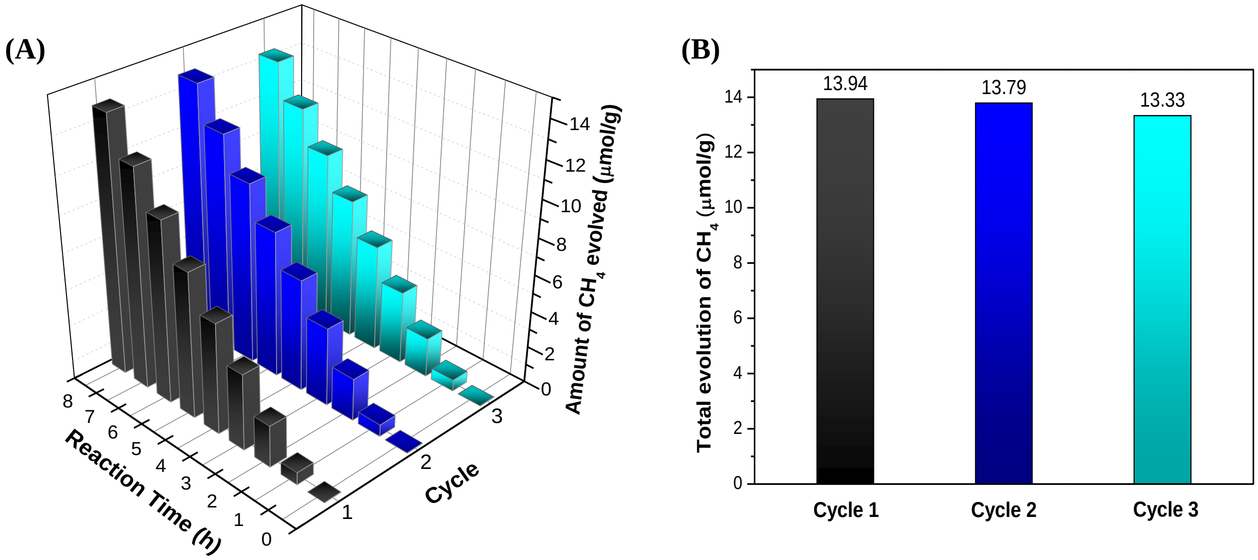

Figure S4 Recycling runs of photocatalytic CO_2 reduction over Bi_2WO_6-OV under simulated solar light irradiation: (A) Time courses of CH_4 evolution and (B) total CH_4 evolution for each cycle.

References

1 X. Y. Kong, W. P. C. Lee, W.-J. Ong, S.-P. Chai and A. R. Mohamed, *ChemCatChem*, 2016, **8**, 3074.

2 W.-J. Ong, L.-L. Tan, S.-P. Chai, S.-T. Yong and A. R. Mohamed, *Nano Energy*, 2015, **13**, 757.

3 W.-J. Ong, L.-L. Tan, S.-P. Chai and S.-T. Yong, *Chem. Commun.*, 2014, **51**, 858.

4 W.-J. Ong, L.-L. Tan, S.-P. Chai, S.-T. Yong and A. R. Mohamed, *Nano Res.*, 2014, **7**, 1528.

5 L.-L. Tan, W.-J. Ong, S.-P. Chai and A. R. Mohamed, *Chem. Commun.*, 2014, **50**, 6923.

6 L.-L. Tan, W.-J. Ong, S.-P. Chai and A. R. Mohamed, *Appl. Catal. B Environ.*, 2015, **166**–**167**, 251.